Heterogeneous ensemble selection for evolving data streams. [Dataset]

LUONG, A.V., NGUYEN, T.T., LIEW, A.W.-C. and WANG, S.

2021

Supplementary Material:

Heterogeneous Ensemble Selection for Evolving Data Streams

Anh Vu Luong[1], Tien Thanh Nguyen[2], Alan Wee-Chung Liew[1], Shilin Wang[3]
[1] School of Information and Communication Technology, Griffith University, Australia
[2] School of Computing Science and Digital Media, Robert Gordon University, Aberdeen, Scotland, UK
[3] School of Electronic Information and Electrical Engineering, Shanghai Jiaotong University, China

Table S1. CPU Running Time – immediate setting

Dataset name	OzaBagAdwin	OzaBoostAdwin	BOLE	BLAST	EFDT	MajorityVoteAdwin	HEES
20_newsgroups	522.3591 (4)	1,235.3702 (6)	633.1091 (5)	1,777.3947 (7)	294.0706 (1)	362.9933 (3)	337.3328 (2)
Electricity	4.1620 (5)	26.2616 (7)	11.7974 (6)	3.8556 (4)	2.6013 (2)	2.7147 (3)	2.4748 (1)
KDDCup99_full	909.0535 (5)	970.2646 (6)	539.7929 (3)	3,857.5166 (7)	633.0595 (4)	459.0883 (2)	453.8868 (1)
Adult	8.8633 (5)	45.6118 (7)	12.7915 (6)	4.5970 (2)	2.2364 (1)	5.7904 (4)	5.1638 (3)
Vehicle	119.7422 (5)	1,016.2150 (7)	211.2450 (6)	103.1140 (2)	28.1336 (1)	115.4479 (3)	119.6607 (4)
Cod-rna	119.1243 (4)	810.9616 (7)	131.3955 (6)	103.0746 (2)	25.7449 (1)	117.0976 (3)	128.0034 (5)
IMDB-F.drama	834.0441 (2)	17,406.2467 (7)	2,600.3884 (5)	2,726.5657 (6)	706.5368 (1)	1,109.1813 (3)	1,353.9509 (4)
Covtype	173.5101 (4)	9,668.6344 (7)	421.8521 (5)	455.9274 (6)	80.0691 (1)	134.6431 (3)	116.7310 (2)
Agrawal	360.7926 (5)	6,041.6090 (7)	728.1515 (6)	169.1566 (2)	40.2542 (1)	181.0391 (3)	222.2868 (4)
AssetNegotiation-F2	365.0761 (6)	6,487.0020 (7)	362.7958 (5)	195.1397 (3)	37.9908 (1)	192.5732 (2)	195.3374 (4)
AssetNegotiation-F3	316.0701 (5)	4,262.7281 (7)	381.1593 (6)	170.0778 (2)	36.2758 (1)	175.5424 (3)	180.2058 (4)
AssetNegotiation-F4	289.2213 (5)	5,962.3460 (7)	458.5207 (6)	191.4152 (4)	40.4094 (1)	170.2905 (2)	171.3755 (3)
BNG_tic-tac-toe	3.7668 (5)	18.8834 (7)	6.0735 (6)	1.6780 (2)	2.3779 (4)	1.8729 (3)	1.5274 (1)
BNG_vote	15.5049 (5)	84.8789 (7)	19.2577 (6)	8.7521 (2)	4.2910 (1)	10.9598 (4)	10.5136 (3)
BNG_trains	1,407.5759 (5)	8,832.8828 (7)	1,529.8782 (6)	756.7747 (2)	133.8136 (1)	785.3134 (3)	856.5607 (4)
BNG_soybean	503.0540 (2)	17,402.8365 (7)	595.9524 (3)	1,199.7171 (6)	396.2508 (1)	1,034.2631 (5)	1,013.6974 (4)
BNG_mushroom	1,432.8789 (5)	4,396.3173 (7)	1,647.8042 (6)	648.5933 (3)	116.4900 (1)	669.9975 (4)	635.0060 (2)
BNG_kr-vs-kp_small	1,001.1264 (6)	5,952.2283 (7)	424.3454 (2)	496.9197 (3)	81.9876 (1)	534.0768 (4)	617.1357 (5)
BNG_segment	359.3403 (6)	2,562.1331 (7)	339.1186 (5)	221.2855 (2)	72.4050 (1)	247.1701 (3)	271.7858 (4)
BNG_ionosphere	1,317.8708 (5)	10,261.7678 (7)	1,564.2149 (6)	705.8061 (3)	137.8421 (1)	815.7916 (4)	676.4537 (2)
BNG_credit-g	1,459.7512 (6)	22,075.9436 (7)	1,225.0100 (5)	699.8195 (2)	133.8246 (1)	791.0822 (4)	768.7749 (3)
BNG_SPECT	593.0257 (6)	12,174.0188 (7)	273.6120 (2)	349.8870 (4)	57.9322 (1)	414.7667 (5)	346.8028 (3)

BNG_solar-flare	251.4346 (5)	1,789.5156 (7)	292.4370 (6)	133.3554 (3)	42.7450 (1)	168.5887 (4)	132.8174 (2)
BNG_page-blocks	34.7971 (4)	1,018.1985 (7)	40.6930 (6)	30.8410 (2)	11.0001 (1)	39.3484 (5)	33.6819 (3)
BNG_lymph	361.9257 (6)	6,570.7449 (7)	208.0189 (2)	268.9203 (4)	86.7093 (1)	320.0481 (5)	250.0566 (3)
BNG_labor	671.4778 (6)	7,017.9531 (7)	639.1828 (5)	399.5729 (4)	76.4718 (1)	352.7459 (3)	329.7672 (2)
BNG_hepatitis	628.6571 (6)	12,563.4778 (7)	264.2102 (2)	462.7729 (5)	62.0467 (1)	425.2032 (4)	414.1205 (3)
BNG_heart-statlog	638.3915 (6)	10,746.0896 (7)	343.4687 (2)	400.5669 (3)	66.0761 (1)	406.5808 (4)	407.5827 (5)
BNG_heart-c	233.7623 (6)	5,999.1861 (7)	192.6437 (5)	139.2280 (2)	53.9405 (1)	156.1082 (3)	156.9938 (4)
BNG_dermatology	218.2174 (2)	6,865.9497 (7)	305.2161 (3)	445.5487 (6)	182.2661 (1)	345.8249 (4)	356.2272 (5)
BNG_credit-a	1,141.8048 (6)	11,126.8761 (7)	856.3911 (5)	690.3159 (2)	98.5155 (1)	736.6221 (3)	806.1008 (4)
BNG_spambase	1,553.8489 (3)	16,298.8009 (7)	1,232.8859 (2)	3,354.7292 (6)	96.0143 (1)	1,797.5517 (4)	1,927.9050 (5)
BNG_optdigits	527.0065 (2)	10,168.8204 (7)	569.0506 (4)	3,150.6129 (6)	557.0688 (3)	611.0266 (5)	508.2674 (1)
BNG_anneal	1,115.0257 (5)	9,342.5161 (7)	1,481.7488 (6)	1,063.5185 (4)	139.0807 (1)	586.7907 (2)	940.0922 (3)
BNG_wine	366.4213 (4)	3,779.2347 (7)	217.9657 (2)	649.4427 (6)	61.1157 (1)	349.5678 (3)	601.8777 (5)
BNG_waveform-5000	1,027.9339 (5)	23,507.8072 (7)	752.5091 (2)	1,284.5588 (6)	155.3863 (1)	766.6441 (3)	857.2880 (4)
BNG_sonar	3,041.5386 (5)	59,226.4058 (7)	1,766.2272 (2)	3,586.5063 (6)	200.5463 (1)	1,925.3127 (3)	1,970.1261 (4)
BNG_satimage	684.9374 (3)	2,079.3619 (7)	845.3692 (4)	928.9844 (5)	130.6844 (1)	605.3314 (2)	1,120.4138 (6)
BNG_cmc	4.8755 (6)	4.5041 (5)	7.5019 (7)	2.0314 (2)	1.4294 (1)	2.6083 (3)	2.6686 (4)
Hyperplane_10_1E-4	433.6528 (5)	7,023.3880 (7)	398.8198 (4)	457.3916 (6)	42.7962 (1)	102.4623 (2)	112.2725 (3)
Hyperplane_10_1E-3	136.7160 (4)	10,808.6357 (7)	259.1633 (5)	299.9054 (6)	53.4481 (1)	78.8633 (2)	80.6341 (3)
LED_50000	213.5015 (4)	7,453.0017 (7)	218.6946 (5)	477.9442 (6)	57.5332 (1)	112.4055 (2)	112.8618 (3)
RandomRBF_50_1E-4	179.1694 (4)	11,507.8654 (7)	276.7359 (5)	574.9665 (6)	104.8372 (3)	88.8679 (1)	98.0227 (2)
RandomRBF_50_1E-3	181.5932 (4)	72,719.8469 (7)	402.5640 (6)	217.0652 (5)	54.0522 (1)	76.2865 (2)	92.4584 (3)
RandomRBF_0_0	289.7148 (3)	1,898.0216 (7)	356.9417 (5)	433.8641 (6)	81.4925 (1)	227.0987 (2)	316.3430 (4)
SEA_50000	116.8582 (5)	11,140.4654 (7)	106.2496 (4)	123.4292 (6)	30.1542 (1)	75.1175 (2)	76.9456 (3)
SEA_50	144.0532 (5)	8,409.0089 (7)	94.2942 (4)	264.7587 (6)	30.3455 (1)	72.0572 (2)	72.5741 (3)
Stagger3	34.9187 (6)	23.3638 (5)	37.0899 (7)	15.4682 (1)	18.2379 (2)	22.0604 (3)	22.1227 (4)
Stagger2	38.2253 (6)	26.7180 (5)	42.6985 (7)	18.6907 (1)	22.1784 (2)	25.9364 (4)	25.5910 (3)
Stagger1	35.3560 (6)	25.7595 (5)	37.9135 (7)	16.0283 (1)	18.1660 (2)	23.8946 (4)	22.9260 (3)
Average Ranking	4.76	6.8	4.72	3.96	**1.28**	3.18	3.3
Mean ± Std	528.4346 ±573.53	9,136.7332 ±13,166.89	527.2990 ±558.44	694.7617 ±970.47	**111.9787** **±152.47**	376.6530 ±422.05	406.6681 ±461.83

Table S2. RAM-Hour – immediate setting

Dataset name	OzaBagAdwin	OzaBoostAdwin	BOLE	BLAST	EFDT	MajorityVoteAdwin	HEES
20_newsgroups	6.4561E-04 (4)	1.6681E-02 (6)	9.3970E-04 (5)	3.9524E-02 (7)	2.6522E-04 (1)	3.6809E-04 (3)	3.3303E-04 (2)
Electricity	2.6330E-07 (4)	6.2613E-05 (7)	1.0527E-06 (5)	1.5006E-06 (6)	8.1352E-08 (1)	2.1992E-07 (3)	2.0151E-07 (2)
KDDCup99_full	6.9862E-04 (4)	1.6403E-03 (6)	1.2659E-04 (3)	2.1005E-02 (7)	7.2028E-04 (5)	6.2435E-05 (2)	6.0137E-05 (1)
Adult	6.2167E-06 (6)	2.6894E-04 (7)	3.3719E-06 (3)	2.9661E-06 (2)	2.3087E-07 (1)	3.8194E-06 (5)	3.3914E-06 (4)
Vehicle	4.3470E-04 (3)	6.9618E-02 (7)	1.0529E-04 (2)	4.8272E-04 (4)	9.0426E-06 (1)	5.3280E-04 (5)	5.5558E-04 (6)
Cod-rna	1.4691E-04 (3)	9.5126E-03 (7)	9.3462E-05 (2)	1.9257E-04 (4)	4.1586E-06 (1)	2.2112E-04 (5)	2.3984E-04 (6)
IMDB-F.drama	1.1961E-03 (1)	1.6651E+00 (7)	1.7973E-02 (5)	2.9444E-01 (6)	1.4945E-02 (3)	1.2634E-02 (2)	1.5073E-02 (4)
Covtype	1.8221E-05 (3)	1.1534E+00 (7)	5.7208E-05 (4)	3.2732E-03 (6)	7.1942E-05 (5)	1.7980E-05 (2)	1.6034E-05 (1)
Agrawal	8.1733E-04 (5)	2.4774E-01 (7)	2.8917E-03 (6)	3.1297E-04 (2)	6.6042E-06 (1)	3.4475E-04 (3)	4.2724E-04 (4)
AssetNegotiation-F2	9.4121E-04 (6)	2.9779E-01 (7)	8.4675E-04 (5)	3.2789E-04 (2)	7.7120E-06 (1)	4.5724E-04 (3)	4.6197E-04 (4)
AssetNegotiation-F3	7.5143E-04 (5)	1.3489E-01 (7)	8.4307E-04 (6)	2.7103E-04 (2)	7.3337E-06 (1)	3.9120E-04 (3)	4.0549E-04 (4)
AssetNegotiation-F4	5.6019E-04 (5)	2.2624E-01 (7)	1.2834E-03 (6)	2.6075E-04 (2)	8.3555E-06 (1)	3.2313E-04 (3)	3.2563E-04 (4)
BNG_tic-tac-toe	3.1490E-07 (5)	4.6060E-05 (7)	5.9750E-07 (6)	2.1297E-07 (2)	2.2955E-08 (1)	2.4720E-07 (4)	2.1621E-07 (3)
BNG_vote	5.0302E-06 (6)	3.3570E-04 (7)	3.4872E-06 (2)	3.6700E-06 (3)	1.3000E-07 (1)	4.5995E-06 (5)	4.4110E-06 (4)
BNG_trains	1.2662E-02 (6)	8.6387E-01 (7)	1.0656E-02 (5)	6.4788E-03 (2)	1.4847E-04 (1)	6.6820E-03 (3)	7.4162E-03 (4)
BNG_soybean	1.5023E-04 (2)	2.7217E+00 (7)	1.3717E-04 (1)	1.4228E-02 (6)	1.4321E-03 (3)	9.9229E-03 (5)	9.8134E-03 (4)
BNG_mushroom	1.3423E-02 (6)	1.5297E-01 (7)	1.3404E-02 (5)	4.7053E-03 (3)	1.1875E-04 (1)	4.9066E-03 (4)	4.6100E-03 (2)
BNG_kr-vs-kp_small	6.2445E-03 (6)	2.4967E-01 (7)	6.2533E-04 (2)	2.7788E-03 (3)	3.7415E-05 (1)	2.9875E-03 (4)	3.4604E-03 (5)
BNG_segment	6.5508E-04 (6)	4.2013E-02 (7)	3.8447E-04 (2)	4.6562E-04 (3)	2.4363E-05 (1)	5.3427E-04 (4)	5.8380E-04 (5)
BNG_ionosphere	1.1330E-02 (5)	7.5046E-01 (7)	1.1418E-02 (6)	5.6854E-03 (3)	1.3121E-04 (1)	6.4285E-03 (4)	5.2630E-03 (2)
BNG_credit-g	1.4164E-02 (6)	3.1316E+00 (7)	7.6835E-03 (5)	5.9850E-03 (2)	1.5055E-04 (1)	6.5998E-03 (4)	6.4853E-03 (3)
BNG_SPECT	2.1534E-03 (6)	1.1282E+00 (7)	2.1894E-04 (2)	1.4324E-03 (4)	1.5100E-05 (1)	1.6703E-03 (5)	1.3914E-03 (3)
BNG_solar-flare	3.8344E-04 (5)	2.4787E-02 (7)	3.9207E-04 (6)	1.8461E-04 (3)	6.7816E-06 (1)	2.3287E-04 (4)	1.8183E-04 (2)
BNG_page-blocks	1.0644E-05 (3)	2.6084E-02 (7)	4.1657E-06 (2)	1.2473E-05 (4)	3.3353E-07 (1)	1.5907E-05 (6)	1.3538E-05 (5)
BNG_lymph	7.9357E-04 (5)	3.3602E-01 (7)	5.6553E-05 (2)	7.6775E-04 (4)	4.3270E-05 (1)	9.0763E-04 (6)	7.0261E-04 (3)
BNG_labor	2.8945E-03 (6)	3.9648E-01 (7)	2.0146E-03 (5)	1.8355E-03 (4)	3.3202E-05 (1)	1.4453E-03 (3)	1.3348E-03 (2)
BNG_hepatitis	2.4809E-03 (6)	1.0294E+00 (7)	1.5887E-04 (2)	2.4720E-03 (5)	1.5462E-05 (1)	1.9745E-03 (4)	1.9354E-03 (3)
BNG_heart-statlog	2.6980E-03 (6)	8.7195E-01 (7)	4.0401E-04 (2)	1.8472E-03 (3)	2.0772E-05 (1)	1.8553E-03 (4)	1.8683E-03 (5)
BNG_heart-c	2.4559E-04 (6)	1.5290E-01 (7)	1.9731E-05 (2)	1.7091E-04 (3)	9.5178E-06 (1)	1.8918E-04 (4)	1.9188E-04 (5)
BNG_dermatology	2.2204E-05 (1)	4.6662E-01 (7)	9.7497E-05 (2)	2.0446E-03 (6)	2.5337E-04 (3)	1.1726E-03 (4)	1.2106E-03 (5)

BNG_credit-a	8.5937E-03 (6)	1.0732E+00 (7)	3.0404E-03 (2)	5.4787E-03 (3)	7.3443E-05 (1)	5.7943E-03 (4)	6.3897E-03 (5)
BNG_spambase	1.1754E-02 (3)	4.4273E-01 (7)	5.5320E-03 (2)	2.5213E-02 (6)	2.8485E-05 (1)	1.3034E-02 (4)	1.4147E-02 (5)
BNG_optdigits	9.9704E-05 (1)	6.8477E-01 (7)	1.5087E-04 (2)	4.8867E-02 (6)	2.9170E-03 (5)	2.6345E-03 (4)	2.2606E-03 (3)
BNG_anneal	7.4723E-03 (5)	6.1336E-01 (7)	1.0787E-02 (6)	6.0401E-03 (4)	1.3842E-04 (1)	3.2702E-03 (2)	5.3602E-03 (3)
BNG_wine	7.8288E-04 (3)	9.6184E-02 (7)	4.5131E-05 (2)	1.9585E-03 (6)	1.7197E-05 (1)	9.7007E-04 (4)	1.6762E-03 (5)
BNG_waveform-5000	5.8974E-03 (5)	4.5561E+00 (7)	7.9020E-04 (2)	8.0988E-03 (6)	1.3202E-04 (1)	4.2810E-03 (3)	4.8732E-03 (4)
BNG_sonar	5.9478E-02 (5)	1.0094E+01 (7)	8.5044E-03 (2)	7.7804E-02 (6)	2.6067E-04 (1)	3.5944E-02 (3)	3.7170E-02 (4)
BNG_satimage	1.5763E-03 (3)	2.6649E-02 (7)	7.9454E-04 (2)	3.1687E-03 (5)	8.1489E-05 (1)	1.8167E-03 (4)	3.3923E-03 (6)
BNG_cmc	5.2035E-07 (5)	1.2603E-06 (7)	8.4880E-07 (6)	2.3160E-07 (2)	1.3445E-08 (1)	2.9416E-07 (3)	3.0160E-07 (4)
Hyperplane_10_1E-4	9.7812E-04 (5)	3.6188E-01 (7)	7.1144E-04 (4)	1.0710E-03 (6)	5.7245E-06 (1)	6.9362E-05 (2)	7.7715E-05 (3)
Hyperplane_10_1E-3	3.3731E-05 (4)	7.6745E-01 (7)	1.7146E-04 (5)	1.0779E-03 (6)	1.0204E-05 (1)	1.8924E-05 (2)	1.9289E-05 (3)
LED_50000	3.6030E-05 (3)	4.1235E-01 (7)	3.0852E-05 (2)	9.8934E-04 (6)	9.9995E-06 (1)	4.8215E-05 (4)	4.9133E-05 (5)
RandomRBF_50_1E-4	8.6752E-06 (1)	7.8935E-01 (7)	2.9018E-05 (4)	1.5683E-03 (6)	6.5798E-05 (5)	9.6143E-06 (2)	1.0900E-05 (3)
RandomRBF_50_1E-3	7.4477E-06 (4)	1.5655E+01 (7)	3.0434E-04 (6)	1.5012E-04 (5)	5.4022E-06 (3)	3.5780E-06 (1)	4.7076E-06 (2)
RandomRBF_0_0	3.3225E-04 (2)	2.1481E-02 (7)	3.9369E-04 (3)	8.4294E-04 (6)	3.2538E-05 (1)	4.0066E-04 (4)	5.6174E-04 (5)
SEA_50000	4.3032E-05 (5)	5.8934E-01 (7)	3.4115E-05 (2)	1.7023E-04 (6)	1.6118E-06 (1)	3.8057E-05 (3)	3.9609E-05 (4)
SEA_50	7.8668E-05 (5)	4.1020E-01 (7)	2.7555E-05 (2)	3.6588E-04 (6)	1.8280E-06 (1)	3.6305E-05 (3)	3.7632E-05 (4)
Stagger3	1.1332E-06 (5)	1.6980E-06 (6)	2.5398E-06 (7)	7.7304E-07 (2)	1.3211E-08 (1)	1.1068E-06 (3)	1.1101E-06 (4)
Stagger2	1.5774E-06 (3)	2.2821E-06 (6)	3.4672E-06 (7)	1.2919E-06 (2)	3.6720E-08 (1)	1.7918E-06 (5)	1.7728E-06 (4)
Stagger1	1.3032E-06 (3)	2.0810E-06 (6)	2.9046E-06 (7)	9.2648E-07 (2)	2.1347E-08 (1)	1.3838E-06 (5)	1.3291E-06 (4)
Average Ranking	4.34	6.9	3.72	4.2	**1.48**	3.62	3.74
Mean ± Std	3.4742E-03 ±9.0149E-03	1.0552E+00 ±2.6451E+00	2.0840E-03 ±4.1317E-03	1.1881E-02 ±4.3152E-02	**4.4537E-04 ±2.1422E-03**	2.6252E-03 ±5.7635E-03	2.8089E-03 ±6.0546E-03

Table S3. Accuracy of base classifiers – immediate setting

Dataset name	EFDT	Hoeffding Adaptive Tree	Hoeffding Option Tree	Hoeffding Tree	NaiveBayes	Perceptron	Random Hoeffding Tree	SGD	kNN	RuleClassifier
20_newsgroups	98.3428 (3)	98.9516 (1)	96.2032 (5)	96.0417 (6)	69.7035 (10)	95.2905 (7)	95.1080 (8)	96.3750 (4)	98.7041 (2)	94.9547 (9)
Electricity	80.6431 (3)	83.3863 (1)	82.9251 (2)	79.1954 (4)	73.3625 (8)	79.1578 (5)	74.1989 (7)	57.5764 (10)	78.3788 (6)	73.2080 (9)
KDDCup99_full	99.9053 (3)	99.9076 (2)	99.9050 (4)	99.9030 (5)	95.6028 (8)	19.8474 (9)	99.6065 (6)	0.0648 (10)	99.9762 (1)	96.0707 (7)
Adult	83.8930 (3)	82.9655 (4)	84.2246 (2)	84.3352 (1)	82.4188 (5)	23.9282 (10)	81.2927 (7)	63.5641 (9)	81.9213 (6)	77.1815 (8)
Vehicle	82.8709 (5)	83.2291 (3)	82.6760 (6)	83.1175 (4)	80.7192 (8)	84.5689 (1)	81.8478 (7)	84.1375 (2)	71.2508 (10)	75.3156 (9)
Cod-rna	94.7104 (3)	94.6234 (4)	95.1773 (1)	94.8903 (2)	74.5272 (9)	94.4548 (5)	89.5087 (6)	66.6663 (10)	89.3902 (7)	81.6919 (8)
IMDB-F.drama	63.2175 (5)	63.4921 (3)	62.6701 (7)	63.3019 (4)	60.2072 (10)	61.8009 (8)	63.0042 (6)	63.7948 (1)	60.5827 (9)	63.6931 (2)
Covtype	84.6678 (3)	81.8942 (4)	84.9179 (2)	80.3119 (6)	60.5208 (10)	81.7067 (5)	64.5661 (7)	60.6956 (9)	92.2249 (1)	61.0703 (8)
Agrawal	94.9662 (1)	94.6453 (4)	94.9174 (3)	94.9188 (2)	88.5224 (5)	67.2045 (8)	73.9393 (7)	55.9550 (10)	64.1503 (9)	84.0668 (6)
AssetNegotiation-F2	94.8781 (1)	94.8315 (4)	94.8664 (3)	94.8712 (2)	92.3612 (5)	50.0062 (10)	91.8280 (6)	74.5303 (9)	87.9043 (8)	90.3286 (7)
AssetNegotiation-F3	94.8034 (1)	94.7928 (4)	94.7959 (2.5)	94.7959 (2.5)	92.1964 (5)	73.3859 (10)	90.7221 (6)	88.2660 (7)	84.5614 (9)	87.3497 (8)
AssetNegotiation-F4	94.7103 (1)	94.6991 (4)	94.7032 (2.5)	94.7032 (2.5)	92.5289 (6)	79.0767 (10)	92.6233 (5)	85.6102 (9)	86.8676 (7)	85.8868 (8)
BNG_tic-tac-toe	73.7438 (2)	73.0148 (5)	73.1520 (3.5)	73.1520 (3.5)	71.6507 (6)	64.5151 (10)	68.6735 (7)	65.2873 (9)	74.7726 (1)	68.6049 (8)
BNG_vote	96.4645 (1)	96.4516 (2)	96.3997 (3.5)	96.3997 (3.5)	91.7755 (9)	96.2456 (5)	91.5283 (10)	93.7859 (7)	94.1574 (6)	92.1394 (8)
BNG_trains	93.8651 (2)	93.8088 (4)	93.8640 (3)	93.9080 (1)	88.7015 (6)	87.2095 (7)	85.5685 (9)	86.7086 (8)	92.3405 (5)	81.3438 (10)
BNG_soybean	86.7306 (5)	89.2012 (4)	89.4310 (2.5)	89.4310 (2.5)	90.1925 (1)	86.5066 (6)	72.9742 (8)	4.9311 (10)	82.2169 (7)	46.2884 (9)
BNG_mushroom	98.9246 (1)	98.8834 (4)	98.8999 (2)	98.8977 (3)	92.7366 (7)	63.8356 (10)	95.0818 (6)	91.3354 (8)	96.4090 (5)	88.7580 (9)
BNG_kr-vs-kp_small	95.2751 (1)	95.1389 (2)	95.0852 (3)	95.0740 (4)	85.0984 (9)	93.6117 (5)	87.9019 (7)	89.5489 (6)	85.9152 (8)	83.1963 (10)
BNG_segment	86.8029 (1)	86.4831 (2)	86.3256 (3)	86.3240 (4)	80.6274 (6)	79.9630 (7)	78.3024 (8)	20.6149 (10)	81.1130 (5)	57.2755 (9)
BNG_ionosphere	94.5173 (3)	94.5171 (4)	94.5771 (2)	94.6066 (1)	79.4557 (10)	89.1435 (5)	89.1157 (6)	85.9340 (8)	85.8816 (9)	86.6961 (7)
BNG_credit-g	77.6606 (3)	77.5386 (4)	77.7071 (1)	77.6996 (2)	76.6185 (5)	66.6861 (9)	74.9992 (6)	59.7689 (10)	72.8744 (7)	71.7526 (8)
BNG_SPECT	84.7103 (4)	84.8991 (1)	84.7670 (2)	84.7482 (3)	75.6326 (10)	82.2279 (6)	82.5633 (5)	79.1579 (9)	80.7551 (7)	79.9180 (8)
BNG_solar-flare	77.6665 (1)	77.6463 (4)	77.6587 (2.5)	77.6587 (2.5)	76.7632 (5)	65.9593 (9)	68.4371 (7)	27.8612 (10)	74.5629 (6)	66.8116 (8)
BNG_page-blocks	90.6606 (1)	90.2965 (2)	90.1506 (4)	90.2830 (3)	79.0005 (9)	45.2644 (10)	89.8972 (6)	83.9455 (8)	90.1218 (5)	89.8135 (7)
BNG_lymph	90.4381 (1)	90.3418 (2)	90.2948 (3)	90.2688 (4)	86.1144 (5)	83.9307 (8)	83.9319 (7)	54.3497 (10)	86.1078 (6)	70.1439 (9)
BNG_labor	94.0453 (4)	94.1539 (2)	94.1456 (3)	94.2959 (1)	90.5369 (8)	64.6999 (10)	91.3736 (7)	91.4844 (6)	92.2156 (5)	87.1751 (9)
BNG_hepatitis	91.3487 (4)	91.3959 (3)	91.4518 (2)	91.5203 (1)	87.6984 (7)	78.3404 (10)	88.4415 (6)	83.6625 (9)	88.7305 (5)	83.8670 (8)
BNG_heart-statlog	88.0540 (2)	88.0731 (1)	87.9847 (4)	87.9964 (3)	86.6734 (5)	55.5946 (10)	84.3947 (7)	78.2583 (8)	84.4843 (6)	77.4658 (9)

BNG_heart-c	88.2790 (1)	88.0848 (2)	87.9825 (3)	87.9734 (4)	86.8016 (5)	54.1436 (10)	82.9400 (7)	73.8838 (9)	84.8094 (6)	75.9877 (8)
BNG_dermatology	97.1862 (5)	97.3154 (4)	97.8276 (2.5)	97.8276 (2.5)	98.6178 (1)	53.2853 (9)	83.6119 (7)	46.8498 (10)	96.3520 (6)	74.2728 (8)
BNG_credit-a	87.9261 (2)	87.8978 (3)	87.9355 (1)	87.7788 (4)	83.0828 (7)	56.4182 (10)	85.9516 (6)	65.0218 (9)	85.9896 (5)	80.9026 (8)
BNG_spambase	66.4295 (2)	66.0618 (5)	66.2666 (4)	66.3023 (3)	66.5160 (1)	64.3861 (8)	65.6299 (6)	60.9013 (10)	62.5557 (9)	65.3282 (7)
BNG_optdigits	84.7050 (7)	89.3682 (5)	90.5222 (4)	90.5408 (3)	90.6300 (2)	91.7304 (1)	67.8009 (8)	19.1676 (10)	89.0955 (6)	31.7202 (9)
BNG_anneal	95.1228 (1)	94.6935 (2)	94.4502 (4)	94.4530 (3)	84.6063 (7)	58.5494 (9)	89.1342 (6)	10.8418 (10)	89.1984 (5)	83.9126 (8)
BNG_wine	93.2879 (3)	93.3377 (2)	93.3756 (1)	93.2626 (4)	92.0195 (5)	40.1055 (10)	88.1579 (7)	60.3481 (9)	91.7358 (6)	76.9820 (8)
BNG_waveform-5000	86.7596 (4)	87.2806 (2)	87.2918 (1)	87.2514 (3)	84.6139 (6)	85.7059 (5)	76.2203 (8)	56.8810 (10)	83.0041 (7)	64.0436 (9)
BNG_sonar	79.9985 (3)	79.7949 (4)	80.9470 (1)	80.0186 (2)	75.5282 (7)	77.7117 (5)	75.5389 (6)	72.4903 (9)	74.5263 (8)	69.6837 (10)
BNG_satimage	82.6513 (1)	82.5078 (2)	82.4029 (3)	82.2742 (4)	78.3235 (7)	80.3891 (6)	76.3198 (8)	32.6663 (10)	81.3113 (5)	59.6891 (9)
BNG_cmc	53.0147 (1)	52.6186 (4)	52.7796 (2.5)	52.7796 (2.5)	51.1701 (5)	34.8687 (9)	46.7538 (7)	34.6372 (10)	47.1788 (6)	44.4010 (8)
Hyperplane_10_1E-4	88.9152 (5)	88.6809 (6)	89.1521 (3)	89.0483 (4)	91.2540 (2)	93.6922 (1)	78.0788 (9)	79.5349 (8)	83.2851 (7)	72.9140 (10)
Hyperplane_10_1E-3	81.5866 (4)	86.6892 (2)	79.7136 (5)	78.7627 (6)	70.9097 (8)	91.8188 (1)	68.2099 (10)	71.1002 (7)	83.3298 (3)	70.2460 (9)
LED_50000	69.8808 (4)	73.5273 (1)	70.3983 (3)	69.0237 (5)	53.9617 (7)	73.3122 (2)	37.5639 (9)	11.9304 (10)	64.1666 (6)	39.2171 (8)
RandomRBF_50_1E-4	51.2695 (4)	62.0962 (2)	56.2785 (3)	45.2726 (6)	30.9945 (9)	50.0062 (5)	36.0621 (7)	16.6315 (10)	89.3566 (1)	35.6160 (8)
RandomRBF_50_1E-3	31.8711 (6)	39.1628 (3)	33.9319 (4)	32.2643 (5)	29.1365 (9)	44.5693 (2)	30.5450 (7)	16.6315 (10)	84.0309 (1)	30.4644 (8)
RandomRBF_0_0	86.0732 (2)	84.2427 (3)	83.1780 (5)	83.1890 (4)	51.2079 (8)	52.8404 (7)	71.0141 (6)	16.6315 (10)	88.9888 (1)	50.3018 (9)
SEA_50000	84.8242 (6)	88.3060 (1)	84.9005 (4)	84.8867 (5)	83.8723 (7)	58.3392 (10)	83.1303 (8)	84.9941 (3)	86.3604 (2)	80.5273 (9)
SEA_50	84.9588 (4)	88.8414 (1)	84.8808 (6)	84.8821 (5)	83.8731 (7)	58.3501 (10)	83.1540 (8)	85.5001 (3)	86.8662 (2)	81.4760 (9)
Stagger3	99.9996 (3.5)	99.9995 (6)	99.9996 (3.5)	99.9996 (3.5)	99.9996 (3.5)	99.9992 (7.5)	99.9998 (1)	99.1494 (10)	99.9992 (7.5)	99.9831 (9)
Stagger2	99.9985 (2.5)	99.9984 (4.5)	99.9984 (4.5)	99.9985 (2.5)	99.9990 (1)	88.5570 (10)	99.1740 (8)	88.8150 (9)	99.9978 (6)	99.8367 (7)
Stagger1	99.9990 (3)	99.9971 (6)	99.9990 (3)	99.9990 (3)	99.9991 (1)	99.9983 (5)	99.7680 (9)	98.3285 (10)	99.9970 (7)	99.9053 (8)
Average Ranking	2.84	3.09	3.1	3.34	6.25	7.15	6.96	8.44	5.61	8.22
Mean ± Std	85.6651 ±13.5718	86.3953 ±12.4584	85.8818 ±13.1855	85.4088 ±13.9615	79.7813 ±15.8268	70.4588 ±19.7953	79.1238 ±15.7737	61.9361 ±28.4108	84.2141 ±11.0006	73.7896 ±17.5006

Table S4. Accuracy of best performing HEES, best performing heterogeneous ensemble (BLAST) best performing homogeneous ensemble (OzaBagAdwin), best performing individual learner (EFDT)

Dataset name	OzaBagAdwin	BLAST	EFDT	HEES
20_newsgroups	99.5497	99.5727	98.3428	99.7520
Electricity	84.3485	85.1209	80.6431	87.0101
KDDCup99_full	99.9470	99.9630	99.9053	99.9690
Adult	84.7058	84.3147	83.8930	84.6915
Vehicle	84.2096	84.4846	82.8709	84.8510
Cod-rna	95.5766	95.0698	94.7104	95.5676
IMDB-F.drama	63.0794	63.6128	63.2175	63.7236
Covtype	84.7394	87.3579	84.6678	88.4433
Agrawal	94.9480	94.9616	94.9662	94.9203
AssetNegotiation-F2	94.8739	94.8781	94.8781	94.8793
AssetNegotiation-F3	94.8030	94.8060	94.8034	94.8070
AssetNegotiation-F4	94.7081	94.7128	94.7103	94.7117
BNG_tic-tac-toe	74.0639	73.6016	73.7438	73.7413
BNG_vote	96.5324	96.4874	96.4645	96.5538
BNG_trains	94.2126	93.9019	93.8651	94.3701
BNG_soybean	90.2813	90.1310	86.7306	90.2079
BNG_mushroom	98.9510	98.9140	98.9246	98.9634
BNG_kr-vs-kp_small	95.2423	95.2270	95.2751	95.2980
BNG_segment	86.4928	86.7665	86.8029	86.7249
BNG_ionosphere	95.2660	94.6508	94.5173	95.2053
BNG_credit-g	78.2546	77.6404	77.6606	78.1084
BNG_SPECT	84.9970	84.8693	84.7103	84.9402
BNG_solar-flare	77.6641	77.6443	77.6665	77.6800
BNG_page-blocks	90.4195	90.6393	90.6606	90.5336
BNG_lymph	90.7837	90.4359	90.4381	90.7974
BNG_labor	94.6272	94.2506	94.0453	94.5580
BNG_hepatitis	92.0154	91.4911	91.3487	91.7896
BNG_heart-statlog	88.7972	88.0921	88.0540	88.5871
BNG_heart-c	88.2121	88.1843	88.2790	88.2904
BNG_dermatology	98.5767	98.6070	97.1862	98.6012

BNG_credit-a	88.3241	87.9507	87.9261	88.3288
BNG_spambase	66.5615	66.4993	66.4295	66.5413
BNG_optdigits	90.6541	91.7469	84.7050	91.6997
BNG_anneal	94.8361	95.0877	95.1228	94.9965
BNG_wine	93.9554	93.4094	93.2879	93.8587
BNG_waveform-5000	88.6755	87.3046	86.7596	88.3767
BNG_sonar	82.3031	80.7370	79.9985	81.8965
BNG_satimage	84.0677	82.7787	82.6513	84.3843
BNG_cmc	52.9062	53.1539	53.0147	53.2353
Hyperplane_10_1E-4	90.0683	93.8233	88.9152	92.9739
Hyperplane_10_1E-3	88.3785	91.8482	81.5866	90.9733
LED_50000	73.9247	73.7455	69.8808	73.8981
RandomRBF_50_1E-4	59.3582	64.1603	51.2695	65.5343
RandomRBF_50_1E-3	51.9859	46.0909	31.8711	48.8570
RandomRBF_0_0	87.6844	86.0249	86.0732	86.5998
SEA_50000	88.3789	88.4505	84.8242	88.4440
SEA_50	88.5785	88.9968	84.9588	89.1715
Stagger3	99.9996	99.9996	99.9996	99.9997
Stagger2	99.9988	99.9990	99.9985	99.9990
Stagger1	99.9984	99.9989	99.9990	99.9990
Mean ± Std	87.2303 ±11.6737	87.2439 ±11.8804	85.6651 ±13.5718	**87.5609 ±11.6018**

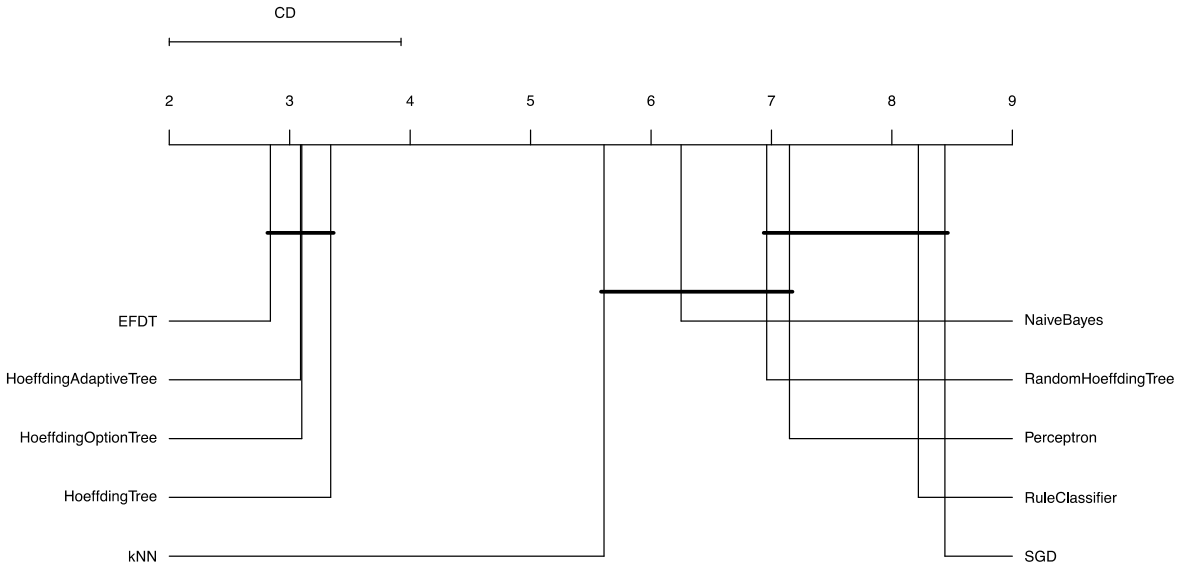

Figure S1. The result of Nemenyi test based on the accuracy of all base classifiers

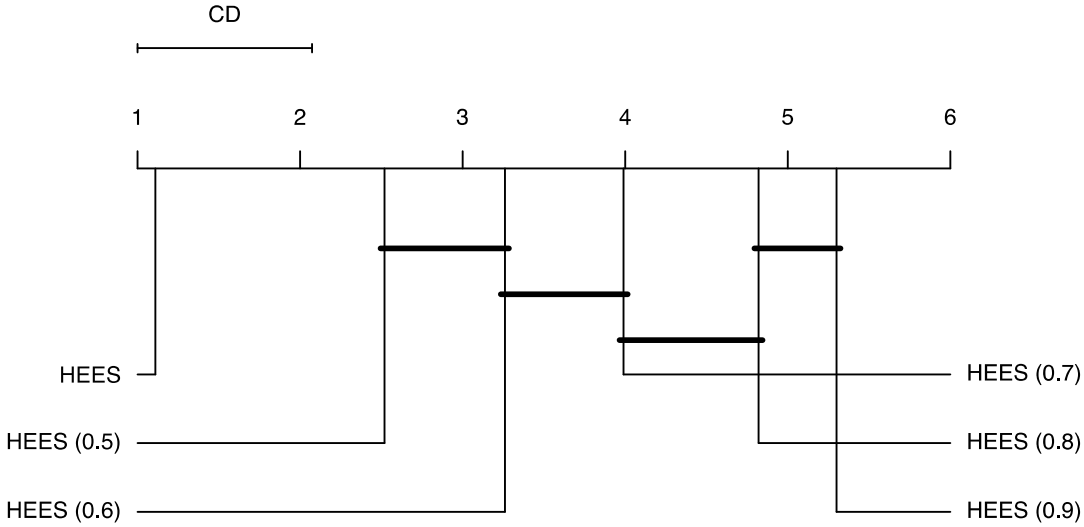

Figure S2. The result of Nemenyi test based on the accuracy of different HEES variants

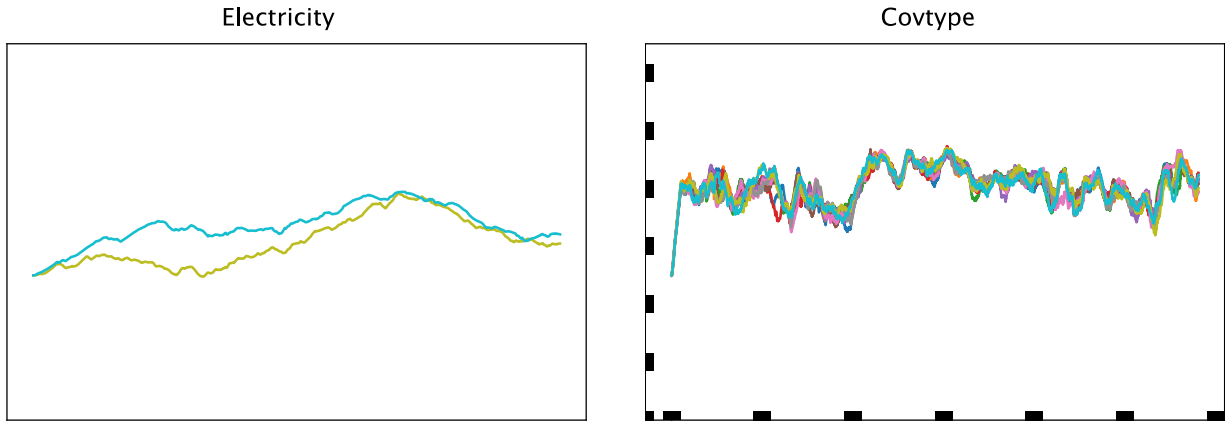

Figure S3. Values of thresholds of the first 10 base classifiers over time for homogeneous ensemble system

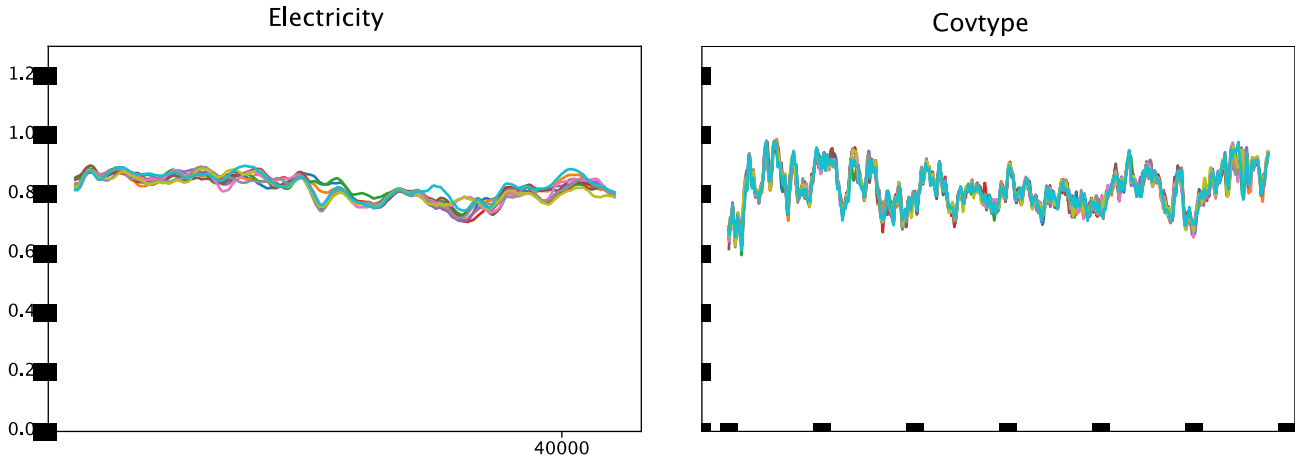

Figure S4. Prequential accuracies of the first 10 base classifiers over time for homogeneous ensemble system

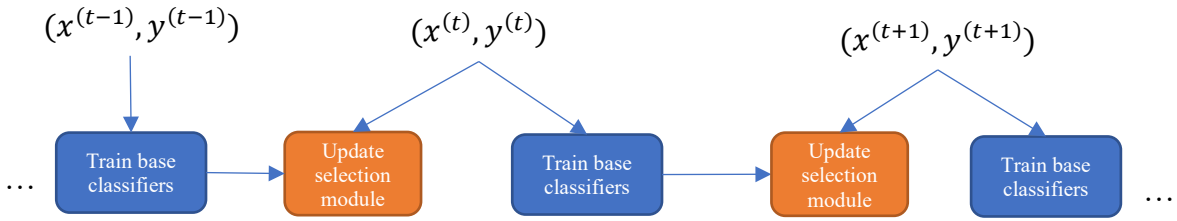

Figure S5. The update process of the proposed framework

Dataset descriptions

20 Newsgroups The original 20 Newsgroup dataset is commonly used in cluster analysis, containing 19,300 newsgroup messages, each represented with 1000 binary attributes (word presence/absence). This dataset is often converted into 20 binary classification problems, one for each newsgroup, and these datasets are then concatenated to form one large binary-class dataset comprising of 386,000 records with 19 shifts in concept.

Electricity This is a real-world dataset containing 45,312 instances coming from the Australian New South Wales Electricity market. The goal is to predict a growth (UP) or a decline (DOWN) in the electricity price. The samples are recorded every 30 minutes over a period of two years. We do not know exactly when drift occurs since this dataset comes from a real-world application.

KDD99: KDD'99 is the dataset used for The Third International Conference and Data Mining Tools Competition, aiming to classify "bad" connections, i.e., intrusions (or attacks) and "good" normal connections. This is a real-world data stream containing 4,898,431 instances, 41 features, and 23 class labels.

Adult The Adult dataset comes from the Census Bureau, and the task is to classify whether a given adult makes over $50,000 a year based on attributes such as age, education, capital gain, capital loss, hours of work per week, etc. This is a binary-class dataset containing 48,842 instances with 14 features.

Cod-rna The Cod-rna dataset contains 488,565 instances with eight different features. The task is to detect non-coding RNAs based on predicted secondary structure formation free energy change. The version used in our experiment is created by joining the test, train, and rest set of the original dataset.

IMDB The IMDB dataset is originally a multi-label dataset derived from the MEKA repository[1], in which each label represents a genre of movies. It was converted to a binary-class data stream by selecting a genre of interest for a user at a particular time, then giving the movies of that genre a positive label. Concept drift is simulated by changes in the genre of interest after some time. Specifically, three changes were introduced in this data stream (after 25, 50, and 75 thousand instances).

CovType The CovType dataset is widely used in the data stream literature, containing 581,012 instances, each of which represents forest cover type for 30 × 30 meter cells acquired from the US Forest Service (USFS) Region 2 Resource Information System (RIS) data. In this dataset, the changes in geographical conditions, e.g., time and weather changes, may lead to concept drift.

Vehicle The Vehicle dataset contains 98,528 silhouettes, each of which has 100 features such as compactness, circularity, distance circularity, etc. Given a silhouette, the goal is to classify it as one of four types of vehicles, which may be viewed from one of many different angles.

Agrawal: The Agrawal generator [Agrawal1993] generates data streams in which each sample is composed of nine features: salary, commission, age, education level, car make, zip-code, house value, years house is owned, and loan value. The task is to determine

[1] https://waikato.github.io/meka/datasets/

whether a bank customer should or should not be given a loan. Ten mapping functions relying on different subsets of the features are used to map instances to 2 possible classes.

Asset Negotiation: The Asset Negotiation generator generates instances in the form of assets with five features: color, price, payment, amount, and delivery delay, aiming to simulate drifting bilateral multi-agent system negotiation of assets. The task is to classify whether an opposing agent is interested in an asset or not. Changes in the interest of an agent are simulated by modifying the concept through time by using five mapping functions relying on different subsets of the features.

Bayesian Network The Bayesian Network Generator builds a Bayesian Network over a batch data and then uses the probability tables to generate instances. In the generated data stream, the concept drift does not exist because the Bayesian Network does not change statistically over time.

Hyperplanes The Rotating Hyperplane Generator [Hulten2001] generates a hyperplane and a stream of points in a high-dimensional space. Here, each instance corresponds to a point, and the goal is to predict whether a certain point is within the hyperplane. By rotating and then changing the position of the hyperplane, the concept drift can be simulated.

LED The LED Generator generates instances whose attributes represent the lights of an LED display. The goal is to predict which digit is depicted by the LED display. Noise can be added by allowing attributes to display the wrong value with a particular probability, or by adding irrelevant attributes.

Random RBF The Random RBF Generator generates several centroids in the Euclidean space. A random weight, standard deviation, and class label are assigned to each centroid. A point in the Euclidean space defines an instance belonging to the class label assigned to the centroid nearby. Gradual concept drift can be simulated by moving the centroids at a certain speed.

SEA Concepts The SEA Concepts Generator generates instances with three attributes. All attributes are numeric values ranging from 0 to 10, and only the first two are relevant. Four concepts are simulated by using different thresholds θ (9, 8, 7, and 9.5), such that $f_1 + f_2 \leq \theta$ where f_1 and f_2 are the first two attributes.

STAGGER The STAGGER Concepts Generator generates instances based on geometrical objects. The attributes of each instance correspond to the size (small, medium, large), color (red, green, blue), and shape (square, circle, triangle) of an object. Three classification problems are given by three decision functions (defined by three STAGGER concepts): $f_1: size = small$ and $color = red$, $f_2: color = green$ or $shape = circle$, and $f_3: size = medium$ or $size = large$.

[Agrawal1993] R. Agrawal, T. Imielinski, A. Swami, Database mining: A performance perspective, IEEE Transactions on Knowledge and Data Engineering. 5 (1993) 914–925.

[Hulten2001] G. Hulten, L. Spencer, P. Domingos, Mining time-changing data streams, in: Proceedings of the Seventh ACM SIGKDD International Conference on Knowledge Discovery and Data Mining, ACM, 2001: pp. 97–106

Delay prequential parameter

To investigate the effect of the delay parameter on the performance of our method and other benchmark algorithms, we examined several values for the delay parameter d (500, 1000, 1500, 2000, 2500, 3000) and computed the accuracy of our method and the benchmark algorithms associated with each value of d. The results in Figure S5 shows that there is a downward trend of the accuracy of all methods with the increase of the delay parameter, and all the lines associated with them shows similar pattern. Therefore, when we compare these methods, the relative rankings of them do not change much especially when the parameter d is greater than or equal to 500. We show the results for the Electricity and the SEA_50000 datasets only in Figure S5, but similar observations hold for almost all other datasets. Therefore, we only report results for the immediate setting ($d = 0$) and the delay setting ($d = 1000$) as commonly used in the literature.

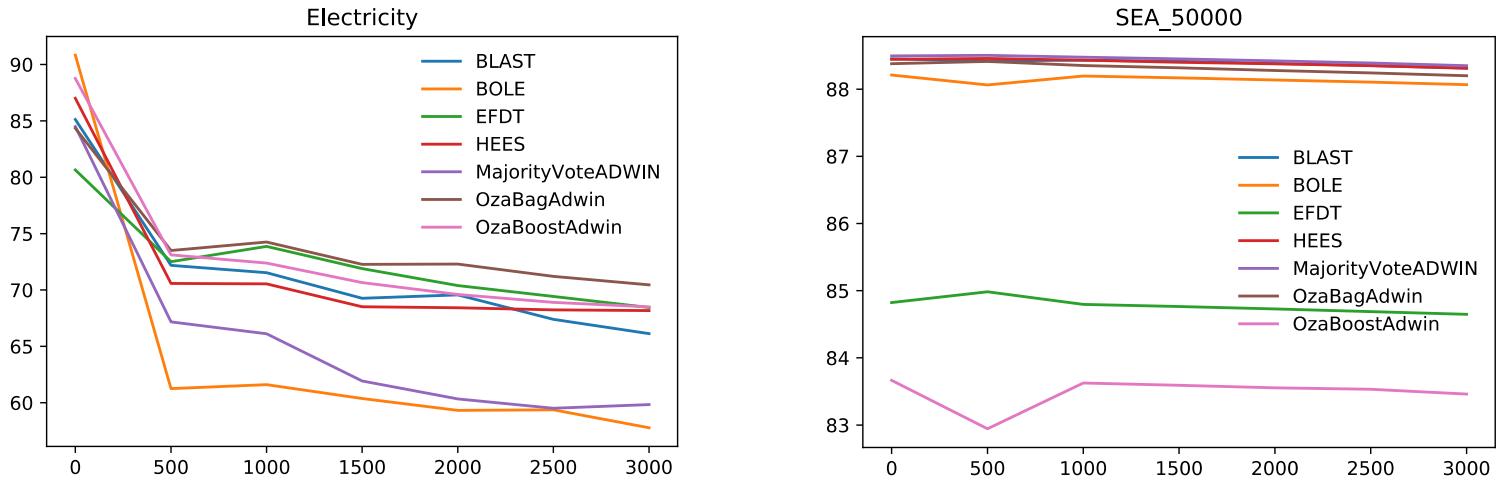

Figure S6. Accuracy on the delay setting with different values of d

Hyper-parameters of the BLAST method

We replicated the experiments in [1] to examine the effect of the Fading Factor α and the number of active classifiers k to the performance of BLAST method on our datasets. Table S5 shows the average accuracy over 50 datasets of different BLAST variants with different values of the Fading Factor and the number of active classifiers. These results support the suggestion of the authors to use the default values of α and k, which are 0.999 and 1, respectively.

Table S5. Average accuracy over 50 datasets of BLAST with different values of α

BLAST ($\alpha = 0.9$)	BLAST ($\alpha = 0.99$)	BLAST ($\alpha = 0.999$)	BLAST ($\alpha = 0.9999$)
86.2375	87.1329	**87.2439**	87.1752

Table S6. Average accuracy over 50 datasets of BLAST with different values of k

BLAST ($k = 1$)	BLAST ($k = 3$)	BLAST ($k = 5$)	BLAST ($k = 7$)
87.1752	87.1369	86.8745	86.6022

[1] van Rijn, J. N., Holmes, G., Pfahringer, B., & Vanschoren, J. (2018). The online performance estimation framework: heterogeneous ensemble learning for data streams. Machine Learning, 107(1), 149-176.